# Operational Characteristics of the Thermally Choked Ram Accelerator

A. P. Bruckner,* C. Knowlen,† A. Hertzberg,‡ and D. W. Bogdanoff§
*University of Washington, Seattle, Washington 98195*

**Operational characteristics of the thermally choked ram accelerator, a ramjet-in-tube device for accelerating projectiles to ultrahigh velocities, are investigated theoretically and experimentally. The projectile resembles the centerbody of a conventional ramjet and travels through a stationary tube filled with premixed gaseous fuel and oxidizer at high pressure. The combustion process travels with the projectile, its thermal choking producing a pressure field which results in thrust on the projectile. The results of experiments with 45–75 gm projectiles in a 12.2 m long, 38 mm bore accelerator, using methane-based propellant mixtures, are presented in the velocity range of 1150–2350 m/s. Acceleration of projectiles with staged propellants and transitions between different mixtures are investigated and the velocity limits in several propellant mixtures are explored. Agreement between theory and experiment is found to be very good.**

## Introduction

THE ram accelerator is a ramjet-in-tube concept for efficiently accelerating projectiles to very high velocities.[1–7] Its propulsive cycle is similar to the aerothermodynamic cycle that generates the thrust in a conventional supersonic airbreathing ramjet, however, the device is operated in a somewhat different manner. The projectile resembles the centerbody of a conventional ramjet and travels through a stationary tube filled with a premixed gaseous fuel and oxidizer mixture (Fig. 1a). There is no propellant on board the projectile. The tube acts as the outer cowling of the ramjet and the combustion process travels with the projectile. Several modes of ram accelerator operation, which span the velocity range of ~0.7–12 km/s, and a number of potential applications of the technology, such as hypervelocity impact studies and direct launch of payloads into space, have been studied by the authors.[1–10] The fundamental differences among the various modes lie in the method of heat release and their operational velocity ranges. In this paper only the thermally choked subsonic combustion mode is discussed. Details of the other modes of acceleration and comparisons of their operational characteristics are presented elsewhere.[1,3,4,6,7]

The propulsive cycle of the subsonic combustion, thermally choked ram accelerator drive mode is initiated by injecting the projectile into the accelerator tube by means of a conventional powder or gas gun. The entrance velocity of the projectile and the composition of the pressurized propellant gas mixture in the accelerator tube are chosen so that the initial projectile Mach number is sufficiently high for the diffuser to start (i.e., the Mach number at the diffuser throat is greater than one). Typically, this minimum starting Mach number is in the range of 2.3–2.8, depending on the gas mixture and projectile geometry. The cone angle of the nose (typically 10 deg–15 deg) is such that the system of oblique shocks in the diffuser does not initiate combustion. The normal shock downstream of the diffuser throat renders the flow subsonic. Provided the Mach number is less than about 4.0–4.5, this shock is also not strong enough to spontaneously ignite the gas mixture. Combustion is initiated immediately behind the projectile by either an on-board ignitor or an external ignitor and the base of the projectile acts as a flame holder. The heat release reaches a thermal choking condition at some distance behind the projectile. This stabilizes the normal shock on the projectile, resulting in forward thrust.

A quasi-steady theoretical model of the thermally choked subsonic combustion mode, assuming calorically perfect gases, and the results of low speed (690–1500 m/s) experiments demonstrating proof-of-principle and pressure scaling effects in a single-stage device were presented in Ref. 1. In this paper we present a more rigorous approach to the theoretical modeling of the acceleration process, including a treatment of the effects of projectile acceleration on the gasdynamics, and present the results of experimental investigations on the operational characteristics of the device at velocities up to 2350 m/s in a multistage configuration using methane-based propellant mixtures.

## Theoretical Modeling

In previous work the flow field was assumed to be in steady motion with respect to the projectile and a closed form an-

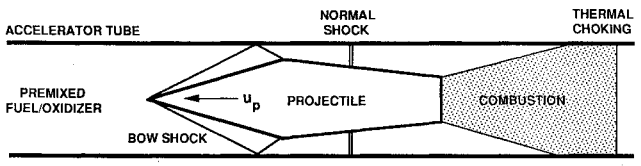


**a) Schematic of projectile accelerating through stationary tube in lab frame of reference**

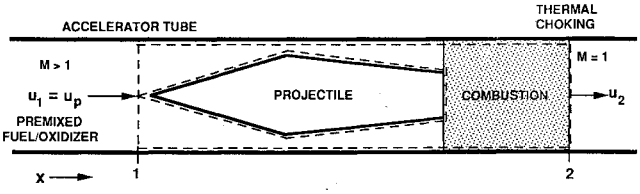


**b) Schematic of idealized model used in analysis; frame of reference moves with projectile**

**Fig. 1 Thermally choked, subsonic combustion ram accelerator.**

Received Aug. 17, 1989; revision received Oct. 31, 1990; accepted for publication Nov. 15, 1990. 

*Research Professor of Aeronautics and Astronautics. Associate Fellow AIAA.

†Graduate Research Assistant, Department of Aeronautics and Astronautics. Student Member AIAA.

‡Professor of Aeronautics and Astronautics; Director, Aerospace and Energetics Research Program. Fellow AIAA.

§Research Engineer, Aerospace and Energetics Research Program; currently Senior Research Scientist, Aerothermodynamics Branch, NASA Ames Research Center, Moffett Field, CA 94035. Member AIAA.

alytical model for the thrust as a function of Mach number was developed, using a one-dimensional (1-D) inviscid approach in which only the initial and end states of the gasdynamic process were considered.[1] In the present work the 1-D approach is generalized by considering the effects of the acceleration of the projectile on the gasdynamics.

Consider a particular instant in time, $t$, at which the projectile is moving at velocity $u_p$, with acceleration $a_p$, to the left in the lab frame (Fig. 1a). A coordinate system is attached to the projectile and positive $x$ is taken to the right in this new frame or reference (Fig. 1b). Combustion is assumed to occur behind the projectile and to result in thermal choking at the full tube area. The control volume used in the analysis is denoted by the dashed lines; it is bounded by Stations 1 and 2, the tube wall, and the projectile. Stations 1 and 2 are, respectively, chosen to coincide with the projectile nose tip and the point at which thermal choking occurs. For simplicity, it is assumed that the location of Station 2 is fixed relative to that of Station 1, i.e., that the control volume is constant. In the projectile frame the propellant moves toward the projectile at velocity $u_1 = u_p$, while accelerating at the rate $\partial u_1/\partial t = a_p$. Because the end state of the process is thermally choked, the thrust on the projectile as a function of its velocity or Mach number can be determined by applying the conservation equations to the control volume, without the need to include any of the internal details of the flow, such as the oblique and normal shock waves or the details of the combustion.[11]

**Continuity**

The time-dependent continuity equation for the control volume is

$$\frac{\partial}{\partial t}\int_{cv} \rho dV = A[\rho_1 u_1 - \rho_2 u_2] \tag{1}$$

where $cv$ indicates integration over the control volume, $\rho$ is the gas density, $V$ denotes volume, $A$ is the cross-sectional area of the tube, and $u$ is the gas velocity relative to the projectile. The subscripts 1 and 2 denote the entrance and exit planes, respectively, of the control volume, where $\rho$ and $u$ are evaluated. The left side of the equation is the rate of accumulation of mass in the control volume as a result of its acceleration. An estimate of the magnitude of this term relative to the convective terms can be obtained by comparing the change in mass flow rate, $\Delta\dot{m}$, entering the control volume during the residence time, $\tau$, of a fluid particle in the control volume to the instantaneous mass flow rate, $\dot{m}_t = \rho_1 u_1 A$, i.e.,

$$\frac{\Delta\dot{m}}{\dot{m}_t} = \frac{\dot{m}_{t+\tau} - \dot{m}_t}{\dot{m}_t} = \frac{\Delta u_1}{u_1} \tag{2}$$

where $\Delta u_1 = a_p\tau$ is the change in the velocity of the incoming flow during $\tau$. The particle residence time can be approximated as $\tau \approx L_{cv}/u_1$, where $L_{cv}$ is the length of the control volume. Thus

$$\frac{\Delta u_1}{u_1} = \frac{a_p L_{cv}}{u_1^2}$$

If the fractional change in projectile velocity during the characteristic residence time of a fluid particle in the control volume is small, i.e., of the order of a few percent or less, the unsteady effects of mass accumulation due to projectile acceleration can be ignored. From numerous experiments it appears that the combustion is completed within approximately one projectile length behind the base of the projectile; therefore, the length of the control volume can be approximated as twice the length of the projectile, i.e., $L_{cv} \approx 2L_p$. Assuming, from typical experimental conditions, that $L_p \approx 150$ mm, $u_1 = 2000$ m/s, and $a_p = 1.5 \times 10^5$ m/s$^2$ (i.e., ~15,000 g), yields a value of ~0.01 for the ratio in Eq. (2). Consequently, the effect of unsteady mass accumulation within the control volume is of little consequence and Eq. (1) reduces to its steady-state form

$$\rho_1 u_1 = \rho_2 u_2 \tag{3}$$

It should be noted that this result states only that the mass flux entering the control volume is the same as the mass flux leaving at any given instant in time; it does not imply that $\rho u$ remains constant for all time.

**Momentum**

If it is assumed that the flow is frictionless, the time-dependent momentum equation in the accelerating frame of reference is

$$\frac{\partial}{\partial t}\int_{cv} \rho u dV + A[(p_2 + \rho_2 u_2^2) - (p_1 + \rho_1 u_1^2)] - \int_{cv} a_p \rho dV = F \tag{4}$$

where $p$ is the static pressure of the gas and $F$ is the net force exerted by the projectile on the control volume. This force is equal in magnitude to the force exerted on the projectile by the gas, i.e., the thrust. The last term on the left-hand side of this equation has the form of a body force and is a consequence of the acceleration of the frame of reference.[12,13]

The unsteady term on the left-hand side of the momentum equation can be evaluated as follows

$$I_1 = \frac{\partial}{\partial t}\int_{cv} \rho u dV = \int_{cv} u\frac{\partial \rho}{\partial t} dV + \int_{cv} \rho \frac{\partial u}{\partial t} dV$$

Based on the discussion of the continuity equation, it can be shown that

$$\int_{cv} u\frac{\partial \rho}{\partial t} dV \approx u_1 \Delta\dot{m} = a_p \rho_1 A L_{cv}$$

In addition, the second integral in $I_1$ can be approximated as

$$\int_{cv} \rho \frac{\partial u}{\partial t} dV \approx \frac{\partial u_1}{\partial t}\rho_1 A L_{cv} = a_p \rho_1 A L_{cv}$$

Thus

$$I_1 \approx 2a_p \rho_1 A L_{cv} \approx 2m_g a_p$$

where $m_g$ is the mass of gas in the control volume.

The acceleration of the frame of reference is uniform, therefore, the body force term in Eq. (4) reduces to

$$I_2 = \int_{cv} a_p \rho dV = m_g a_p$$

Consequently, $I_1$ and $I_2$ partially cancel, leaving a residual term of magnitude $m_g a_p \approx a_p \rho_1 A L_{cv}$. Compare this term to the smaller of the convective terms, $A(p_1 + \rho_1 u_1^2)$; the ratio is

$$R_M = \frac{a_p \rho_1 A L_{cv}}{A(p_1 + \rho_1 u_1^2)}$$

For all realizable operating conditions, it can be shown that $p_1 < 0.1\,\rho_1 u_1^2$. Hence, $p_1$ can be neglected in the denominator and

$$R_M \approx \frac{a_p L_{cv}}{u_1^2}$$

This is the same ratio that was evaluated in the continuity equation and has the value $R_M \approx 0.01$ for the typical operating conditions considered earlier; thus the sum of the unsteady and body force terms in Eq. (4) can be neglected with respect to $A(p_1 + \rho_1 u_1^2)$. It remains to be determined whether this sum is small compared to $F$. From Newton's law, the thrust can be expressed as $F = m_p a_p$, where $m_p$ is the mass of the projectile. Thus, the ratio $(I_1 - I_2)/F$ is approximately equal to $m_g/m_p$, the ratio of gas to projectile mass in the control volume, which for typical operating conditions is about 0.1. Although this is an order of magnitude larger than $R_M$, it is nevertheless small enough that to a reasonable degree of accuracy $I_1 - I_2$ can be neglected with respect to $F$. The momentum equation consequently reduces to its steady-state form

$$F = A[(p_2 + \rho_2 u_2^2) - (p_1 + \rho_1 u_1^2)] \tag{5}$$

**Energy**

The time-dependent energy equation for the control volume is

$$\frac{\partial}{\partial t}\int_{cv}\left(e + \frac{u^2}{2}\right)\rho dV + A\left[\rho_2 u_2\left(h_2 + \frac{u_2^2}{2}\right) - \rho_1 u_1\left(h_1 + \frac{u_1^2}{2} + \Delta q\right)\right] - \int_{cv} u a_p \rho dV = 0 \tag{6}$$

where $h$ is the specific enthalpy of the gas, $\Delta q$ is the heat release per unit mass and $e$ is the specific internal energy of the gas. The last term on the left is the work resulting from the acceleration of the coordinate system.[12] There is no work term associated with the projectile, because it is stationary with respect to the moving reference frame. We must again make estimates for the integral terms. First consider the conditions at the thermal choking point, where the local Mach number is unity. It can be shown that for typical operating conditions $e_2 \approx u_1^2$. Taking this as a maximum value for $e$ in the unsteady term yields

$$I_3 = \frac{\partial}{\partial t}\int_{cv}\left(e + \frac{u^2}{2}\right)\rho dV \approx \frac{\partial}{\partial t}\int_{cv}\frac{3}{2}u_1^2\,\rho dV \approx \frac{9}{2}\rho_1 u_1 A L_{cv} a_p$$

where the earlier approximation $\int_{cv} \partial\rho/\partial t\, dV \approx a_p \rho_1 A L_{cv}/u_1$ has been used. The acceleration work term in Eq. (6) can be estimated as

$$I_4 = \int_{cv} u a_p \rho dV \approx \rho_1 u_1 A L_{cv} a_p$$

Thus

$$I_3 - I_4 \approx \frac{7}{2}\rho_1 u_1 A L_{cv} a_p$$

Compare this term to $A\rho_1 u_1 (h_1 + u_1^2/2 + \Delta q)$. For typical ram accelerator operating conditions, it can be shown that $h_1 \approx 0.2\, u_1^2$ and $\Delta q \approx u_1^2$. Thus

$$A\rho_1 u_1\left(h_1 + \frac{u_1^2}{2} + \Delta q\right) \approx 1.7\, A\rho_1 u_1^3$$

and

$$R_E = \frac{I_3 - I_4}{A\rho_1 u_1\left(h_1 + \frac{u_1^2}{2} + \Delta q\right)} \approx \frac{2a_p L_{cv}}{u_1^2} = 2R_M$$

Since $R_M$ was estimated to be 0.01, $R_E \approx 0.02$. Note, furthermore, that this estimate used the value of $e$ at the choke point throughout the control volume. Since for the majority of the control volume $e$ is much lower than this value, $R_E$ will actually be much smaller than the above estimate. Accordingly, with a high degree of accuracy the unsteady and acceleration work terms can be neglected and the energy equation reduces to its steady-state form

$$h_1 + \frac{u_1^2}{2} + \Delta q = h_2 + \frac{u_2^2}{2} \tag{7}$$

It is evident from the preceding discussion that the quantity which determines whether the acceleration of the projectile gives rise to significant unsteady flow effects is the ratio

$$R_M = \frac{a_p L_{cv}}{u_1^2}$$

It was shown that the acceleration of the projectile at levels typical of current laboratory practice results in a value $R_M \approx 0.01$, which is negligible. Even for values of $R_M$ two or three times greater, the steady-state conservation equations are applicable, which indicates that the present analysis can be extrapolated to accelerations as high as 30,000–40,000 g.

**Methods of Solution**

Equations (3), (5), and (7), together with the ideal gas law, $p = \rho RT$, and the condition of thermal choking at Station 2, i.e., $M_2 = 1$, provide enough relations to solve this set of equations. A closed form solution for the dimensionless thrust coefficient, $F/p_1 A$, as a function of Mach number can be obtained by assuming that $\Delta q$ = constant and that the gas is calorically perfect, both before and after combustion, i.e., that the enthalpies at Stations 1 and 2 can be written as $h_1 = C_{p1} T_1$ and $h_2 = C_{p2} T_2$, respectively.[1] Denoting the ratios of specific heats at Stations 1 and 2 by $\gamma_1$ and $\gamma_2$, respectively, the resulting equation for the thrust coefficient is

$$\frac{F}{p_1 A} = \frac{\gamma_1 M_1}{\gamma_2}\left\{2\left(\frac{\gamma_2^2 - 1}{\gamma_1 - 1}\right)\left[1 + \frac{\gamma_1 - 1}{2}M_1^2 + \frac{\Delta q}{C_{p1} T_1}\right]\right\}^{1/2} - (1 + \gamma_1 M_1^2) \tag{8}$$

which is the same result as obtained with an *a priori* assumption of steady flow.[1] The heat release of combustion, $\Delta q$, is determined from the difference in the enthalpy of formation between the unreacted propellant mixture and the combustion products in chemical equilibrium at sonic velocity with respect to the projectile. Note that the ratios of specific heats, $\gamma_1$ and $\gamma_2$, are computed from the effective values of the specific heats, based on the calorically perfect assumption. Using Eq. (8), it can be shown that the thrust coefficient reaches zero at a Mach number corresponding to that of a 1-D Chapman-Jouguet detonation wave propagating in the same mixture.[1] Thus, theoretically, every candidate propellant mixture has an upper velocity limit corresponding to its C-J speed.

An alternative and more rigorous approach to modeling the acceleration process is to account for the dependence of heat capacity on local temperature and to include the effect of the increase in projectile velocity on the chemical equilibria of the combustion products. This requires an iterative numerical solution of Eqs. (3), (5), and (7), in which the enthalpies, $h_1$ and $h_2$, are determined as functions of temperature from tabulated JANAF data.[14] The iterative technique begins by computing the chemical equilibria of the combustion products for an assumed static temperature and pressure. The heat release is determined from the predicted combustion products and then the total enthalpy of the flow exiting the control volume (with $u_2$ assumed to equal the local acoustic velocity) is compared with the total enthalpy of the incoming flow. The static temperature guess is then modified to raise or lower the total enthalpy of the gas at Station 2, as required, and the pressure is updated from Eq. (3) to maintain mass conser-

vation. The iterative procedure continues until the total enthalpies are balanced to within the desired tolerance for the given mass flow rate. The thrust is then determined from Eq. (5), once the static temperature and pressure at Station 2 are known. This approach predicts that the amount of heat released by the combustion of the propellant mixture decreases somewhat as the flight Mach number increases, due to dissociation losses.

Figure 2 illustrates plots of the thrust coefficient, $F/p_1A$, as a function of Mach number, for the two theoretical approaches described above for a sample mixture, $2.5CH_4 + 2O_2 + 5.6N_2$, used in the experimental studies. Only the supersonic branches of the solutions are shown. The difference between the two approaches described here is primarily a result of the variation of heat release with projectile Mach number. In the closed form solution a constant $\Delta q$, equal to the value determined by the iterative solution at the C-J detonation velocity, was used. In the iterative approach the heat release, and thus the thrust, is somewhat higher at the lower Mach numbers. The difference in $\Delta q$ between the peak thrust point and the C-J point is ~10% and is due to a change in the chemical equilibria of the combustion products resulting from the different initial conditions. Note that both approaches predict a zero thrust condition at the C-J detonation velocity of the propellant mixture.[1]

The dashed portions of the curves indicate a regime not accessible to experiment because it corresponds to Mach numbers below the minimum necessary to establish supersonic flow at the throat, i.e., for the diffuser to start. At Mach numbers above the minimum required for operation, the thrust decreases with increasing Mach number, reaching zero at the C-J point, as noted earlier. This theoretical limit does not preclude the possibility that velocities exceeding the detonation velocity might be realized in practice, as a result of flow effects which are not included in the model. Examples of the latter are thermal choking or supersonic combustion occurring in the annular space between the projectile and the tube, transient wave phenomena, and 3-D flow effects.

The model described here predicts the same performance regardless of the projectile geometry.[11] In addition, for the same set of operational parameters and initial assumptions, the present model yields the same results as an approach which includes all the flow details. The generality of the solution follows from the fact that the process starts from an equilibrium state at Station 1 and ends at another equilibrium state at Station 2, where the flow is thermally choked and the

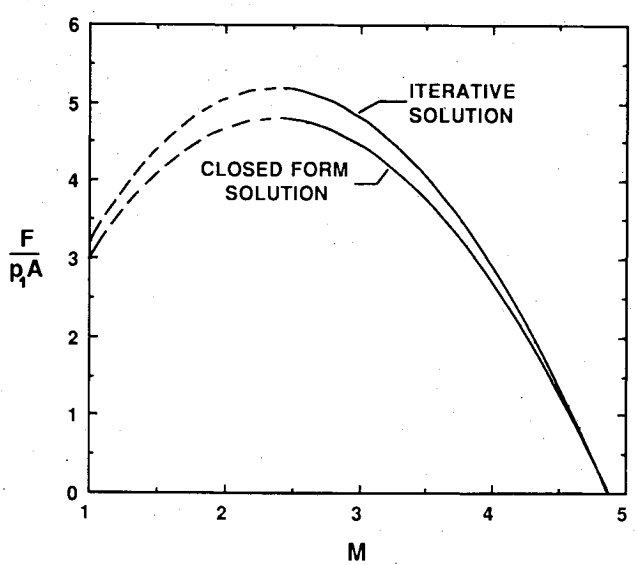


**Fig. 2 Variation of theoretical thrust coefficient with Mach number for $2.5CH_4 + 2O_2 + 5.6N_2$ propellant mixture. Dashed parts of curves denote Mach number regime below minimum required to start diffuser.**

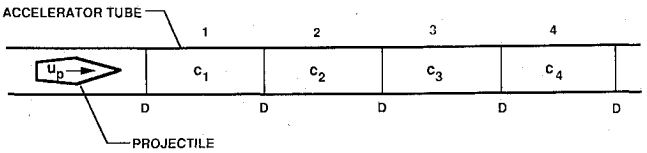


**Fig. 3 Schematic of multi-stage ram accelerator. D denotes diaphragms separating staged propellant mixtures. Pressure is same in all stages. Note that $c_4 > c_3 > c_2 > c_1$, where $c_n$ is the speed of sound in Stage $n$.**

flow area is the same as at Station 1. The end state is always the same for a given heat release and initial Mach number, regardless of the details of the process. In practice, however, the projectile geometry must be such that a normal shock can stand on the projectile somewhere behind the throat. The smallest permissible projectile throat diameter corresponds to the condition where the normal shock is at the throat. The largest throat diameter corresponds to the necessary starting area ratio of the diffuser. In the absence of viscous effects the length of the projectile has no effect on the solution.

Because the theoretical model predicts that a given propellant mixture has a maximum velocity of operation equal to its C-J speed, the acceleration of a projectile to higher velocities can be accomplished, in principle, by filling the tube with a graded propellant mixture whose C-J speed increases towards the muzzle of the tube. Since combustible mixtures with higher C-J speeds tend to have higher acoustic speeds, the projectile can in this manner also be operated over a narrow range of Mach numbers, close to that corresponding to the peak thrust, thus achieving maximum projectile velocity in the shortest possible tube. A more practical approach, shown in Fig. 3, is to divide the tube into several segments, each filled with a different propellant mixture, such that the acoustic and C-J speeds of the mixtures increase towards the muzzle. In this manner, the projectile can be constrained to operate over the optimum Mach number range in each segment, thus permitting the attainment of the desired high velocity with a ram accelerator of reasonable length. This staged propellant approach has been used in the experimental studies to date.

## Ram Accelerator Facility

The ram accelerator facility (Fig. 4) consists of a light gas gun, ram accelerator section, final dump tank, and projectile decelerator. The 38 mm bore single-stage light gas gun is capable of accelerating the projectile and sabot combination (typical combined mass ≈ 60–100 gm) to speeds up to approximately 1350 m/s. The muzzle of the gun is connected to a perforated vent tube that passes through an evacuated tank which serves as a dump for the helium driver gas.

The ram accelerator section consists of seven steel tubes with a bore of 38 mm, an outside diameter of 100 mm, and an overall length of 12.2 m. There are a total of 32 pairs of diametrically opposed instrumentation ports disposed at 28 intervals along the accelerator tube. At four axial stations there are two pairs of opposing ports at right angles to each other, which permits the simultaneous use of four transducers. Piezoelectric pressure transducers are located at each of up to 20 observation ports. The remaining ports are used to mount electromagnetic transducers[15] (copper wire coiled around a stainless steel core) and fiber-optic light guides. A 20-channel, 1 MHz digital data acquisition system (DAS) is used to process the data. Multiplexing permits processing the 50 separate input signals currently being monitored.

The ram accelerator tube is designed to operate at propellant fill pressures up to 50 atm. Thin Mylar diaphragms are used to close off each end and to separate sections of the tube filled with different propellant mixtures. The fuel, oxidizer, and diluent gases are metered using sonic orifices, combined in a mixing chamber, and directed to the various sections of the ram accelerator tube.

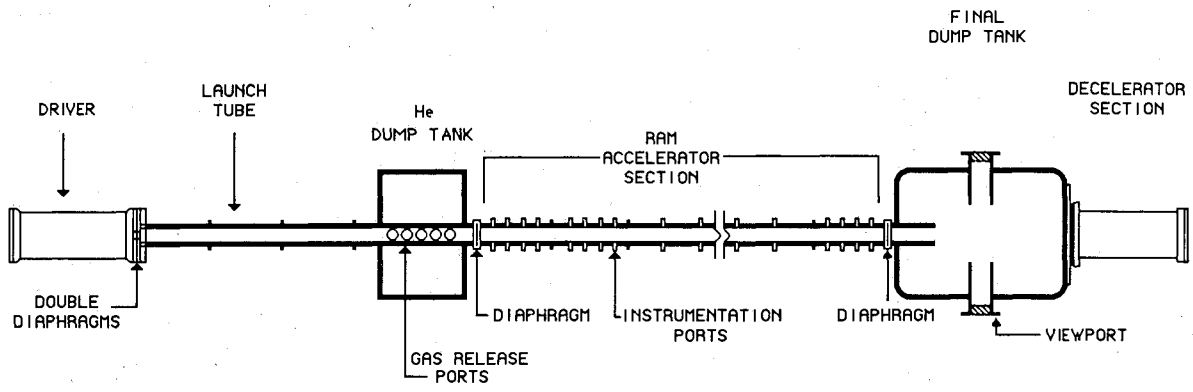


**Fig. 4 Schematic of experimental ram accelerator test facility.**

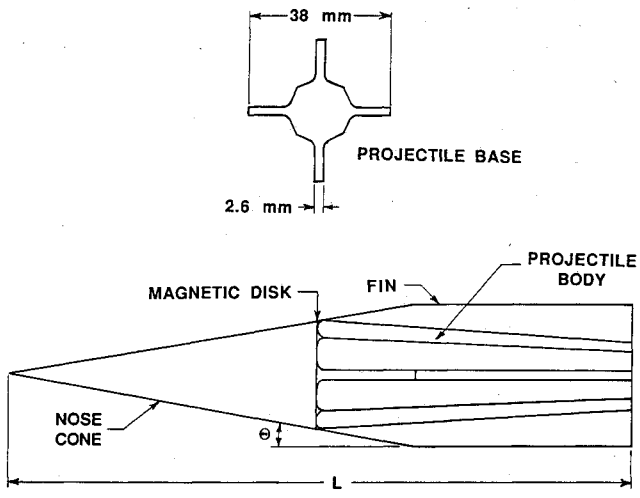


PROJECTILE

| | TYPE A | TYPE B |
|---|---|---|
| L | 138 mm | 166 mm |
| Θ | 12.5° | 10° |

**Fig. 5 Experimental projectile configuration.**

The end of the accelerator tube is connected by a short drift tube to a 2.4 m long evacuated dump tank, where the projectile flies free. The tank has a pair of 25 cm diameter viewing ports for spark photography. The free-flying projectile is brought to a stop in tightly packed rug remnants in an 18 cm I.D. × 1.8 m long tube attached to the far end of the dump tank.

### Projectile Configuration

The basic projectile configuration that has been used in the majority of the experimental work to date is illustrated in Fig. 5. The projectile is fabricated from ZK-60A-T5 magnesium alloy in two separate units: the nose cone and the body with integral fins. The nose and body are hollow. The fins serve only to center the projectile in the tube and the octagonal cross section of the body is a machining convenience. At the threaded joint between the nose and body, there is sandwiched a thin sheet of flexible magnetic material which is shielded from direct contact with the working gas. A second magnet is affixed to the interior of the projectile at its base. These magnets interact with the electromagnetic transducers, providing time of flight data from which the velocity history of the projectile can be determined. The projectile has a maximum body diameter of 28.9 mm. In the 38 mm bore tube the resulting diffuser has a flow area ratio of 2.37.

Two variations of the basic projectile configuration have been used extensively and are referred to in Fig. 5 as Type A and Type B. The differences between the two projectile geometries used lie in the angle of the nose (10 deg and 12.5 deg) and the length of the body (71 mm and 84 mm). The longer body is used with the 10 deg nose. The masses of the projectiles used have been in the range of 45 to 75 gm, depending on the external and internal configurations. The Lexan launching sabot has a mass of 13 gm. A simple ignition system external to the projectile has been developed which eliminates the need for the on-board ignitor charge used in earlier studies.[1] The details of this system are beyond the scope of this paper and will be reported separately at a later date.

## Results and Discussion

### Operating Conditions

Experiments with the thermally choked subsonic combustion ram accelerator mode have been carried out using methane and oxygen as the fuel and oxidizer, and carbon dioxide, nitrogen, helium, and excess methane as the diluents. Several different mixtures, tailored for different operational velocity regimes, have been used. Table 1 lists representative mixtures used by the authors for the present study, together with their acoustic speeds (at 298°K), computed C-J detonation wave speeds (at 25 atm) and corresponding heat release parameters, and observed operational velocity ranges.

Other mixtures have also been investigated.[1,2] The diluents serve to tailor the speed of sound of the mixtures in order to constrain the projectile Mach number to the range of 2.5–4.5, to tune the heat of combustion to a level which stabilizes the normal shock system on the projectile body and to avoid detonation. Propellant fill pressures of 3 to 35 atm absolute and injection velocities in the range of 680–1300 m/s have been investigated in more than 600 test firings to date. To attain velocities in excess of 1700 m/s, the propellant mixtures have been staged, i.e., the ram accelerator tube has been divided into two or more sections containing different propellant mixtures, as noted earlier.

### Transducer Signatures

Figure 6 illustrates typical outputs from an electromagnetic transducer, a pressure transducer, and a fiber-optic light emission probe in a third stage tube segment containing $3.5CH_4 + 2O_2 + 6.5He$ at 25 atm. The transducers are all located 3.96 m from the entrance diaphragm to this stage. The projectile is of the Type B geometry and its velocity and Mach number are 2020 m/s and 3.72, respectively. Time is measured from the instant of DAS triggering and pressure is displayed in units of atmospheres. The zero crossing points of the electromagnetic signal identify the times of arrival of the magnets mounted at the throat and base of the projectile, respectively. These signals provide convenient reference points from which the position of the shock wave system relative to the projectile

**Table 1 Propellant mixtures investigated**

| Propellant composition | $\frac{\Delta q^*}{C_{p1}T_1}$ | Acoustic speed (m/s) | Computed C-J detonation speed (m/s)† | Operational velocity range (m/s) |
|---|---|---|---|---|
| $2.5CH_4 + 2O_2 + 5.6N_2$ | 5.2 | 362 | 1760 | 980–1720 |
| $4.5CH_4 + 2O_2 + 2He$ | 4.7 | 447 | 2070 | 1300–2000 |
| $3.5CH_4 + 2O_2 + 6.5He$ | 3.8 | 543 | 2360 | 1650–2310 |
| $2.8CH_4 + 2O_2 + 11He$ | 3.7 | 622 | 2670 | 1980–2350‡ |

*At Chapman-Jouguet detonation speed.
†$p_1$ = 25 atm, $T_1$ = 298 K.
‡Constrained by length of existing ram accelerator tube.

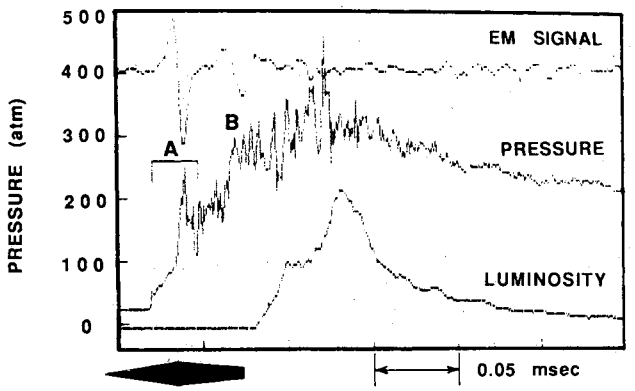


**Fig. 6 Electromagnetic (EM), pressure, and broadband luminosity signals in ram accelerator. Propellant mixture: $3.5CH_4 + 2O_2 + 6.5He$; fill pressure = 25 atm; $u_p$ = 2020 m/s; Type B projectile. Label A denotes oblique shock system in projectile's diffuser section; label B denotes head of normal shock system.**

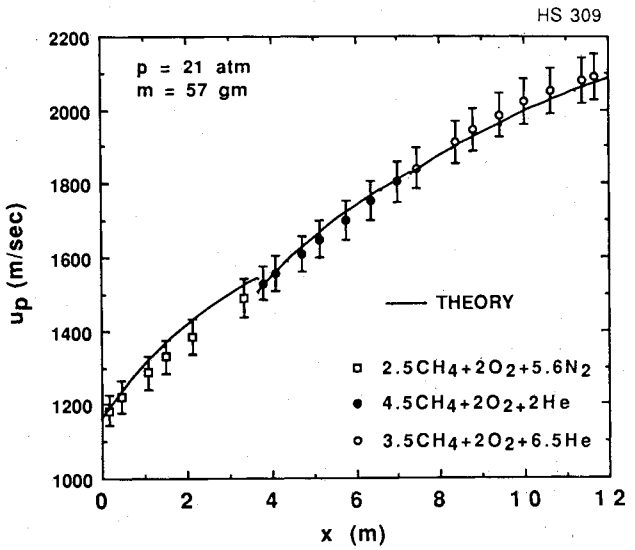


**Fig. 7 Velocity profile in three-stage ram accelerator. Initial velocity = 1150 m/s; projectile mass = 57 gm; propellant fill pressure = 21 atm; Type A projectile.**

can be determined. A profile of the projectile scaled to the local velocity is shown under the transducer signatures in Fig. 6 to illustrate this point.

The first set of pressure pulses, denoted by A in the figure, is generated by the oblique shock system in the projectile's diffuser section. There then follow a series of pulses which increase the pressure to a peak of ~430 atm, after which the pressure decays. There does not appear to be a single, "clean" normal shock. Rather, the increase in pressure after the initial oblique shocks appears to be caused by a complex system of compression waves similar to those observed in the transition of supersonic flows to subsonic in long ducts.[16] The decay in pressure following the peak is assumed to be due to the heat addition choking the subsonic flow and the subsequent nonsteady expansion of the combustion products into the tube downstream of the choking point.

Pressure signatures of both Type A and Type B projectiles observed in other propellant mixtures at equivalent Mach numbers are similar to that of Fig. 6. Although direct experimental confirmation of thermal choking in the flow behind the projectile has not been obtained, its existence is inferred from the fact that the pressure profile remains stable throughout the velocity range of a given mixture. If the flow were not choked, expansion waves from the unsteady flow expansion downstream would catch up to the wave system on the projectile and weaken it, which would result in a rapid loss of thrust.

The fiber-optic probes are used to examine the combustion region and observe the luminosity with respect to projectile position and projectile-generated pressure waves. A typical result is illustrated by the light trace shown in Fig. 6. Since the light detection system is broadband, it is not possible to identify the spectral nature of the light and the chemical species which give rise to the luminosity. However, because the propellant mixtures are methane-rich, it is most likely that the bulk of the luminosity is a result of the presence of molecular carbon ($C_2$ Swan band radiation) and particulate carbon (continuum radiation) in the combustion zone. (Each experimental shot leaves a coating of soot on the walls of the accelerator tube.) Typically, the maximum intensity of the luminosity is located ~3 tube diameters, i.e., less than one projectile length behind the projectile, and somewhat behind the region of peak cycle pressure. Further characterization of the combustion zone will be done at a later time using spectroscopic techniques.

### Velocity Profiles

The velocity of the projectile is deduced from the distance-time history of the electromagnetic transducer signals. The data obtained are curve fit with the highest order polynomial (typically fifth-order) that closely matches the experimental data without producing excessive oscillations in the distance-velocity history which is obtained by differentiation.

Figure 7 shows the in-tube velocity profile obtained in a representative three-stage shot, with a 57-gm Type A projectile and a gas fill pressure of 21 atm. The gas mixtures used are identified in the figure and are similar to the first three listed in Table 1. Each of the three stages was 3.66 m long. The projectile entered the ram accelerator tube at 1150 m/s. The solid curves represent the predicted velocity profiles in each stage and the plotted points the velocities determined from the experimental data at each of the instrument stations. The theoretical curves are initiated at the experimentally determined velocities at the beginning of each propellant mixture. Consequently, these curves are discontinuous relative to each other because theory and experiment do not match exactly at the end of each stage. A peak in-tube velocity of 2130 m/s was obtained with this configuration and the average acceleration level was 15,000 g. It can be seen that the velocity profile of the projectile predicted by the theoretical model is

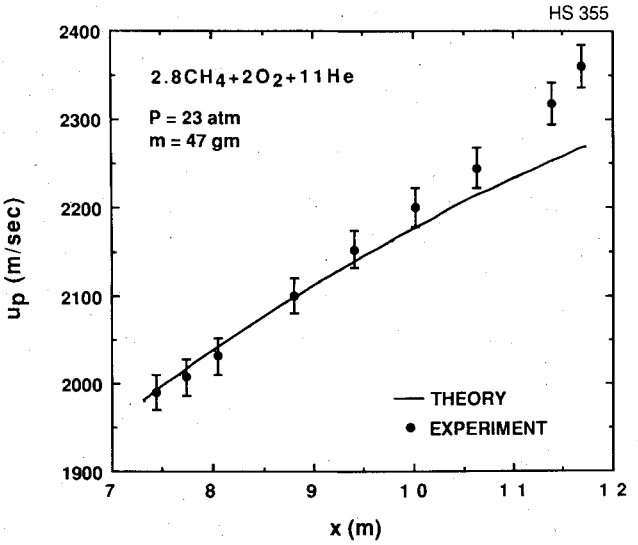


**Fig. 8 Velocity profile in the final stage of a four-stage ram accelerator. Stage entrance velocity = 1980 m/s; projectile mass = 47 gm; propellant fill pressure = 23 atm; Type A projectile.**

in close agreement with experiment throughout the velocity range shown.

Figure 8 shows the velocity profile in the last stage of an experiment conducted with a 47-gm Type A projectile in which the ram accelerator tube was partitioned into four stages, each at 23 atm fill pressure. The fourth stage was 4.6 m long. The projectile was accelerated through three propellant mixtures similar to those shown in Fig. 7 to a velocity of 1980 m/s before entering the fourth stage mixture shown in Fig. 8. The total length of ram accelerator used was 12.2 m. A maximum in-tube velocity of 2350 m/s and a peak acceleration of 30,000 g were observed in the fourth stage. The experimental data from much of this stage lie above the theoretical curve. This behavior has been repeatedly observed and may be caused by combustion beginning to occur on the body of the projectile.

### Operating Limits

As noted earlier, the ram accelerator projectile experiences positive thrust in a given propellant mixture if its velocity lies between the limits imposed by the requirements for the diffuser to start and for the normal shock system to be on the projectile body. If the projectile enters a mixture at too low a velocity, the diffuser unstarts. An unstart condition can also result if the projectile enters a propellant mixture at a Mach number high enough for the diffuser to remain supersonic, yet too low for the area contraction at the throat to be sufficient to contain the normal shock system on the back half of the projectile, i.e., if the heat release of the propellant mixture is too great for the projectile's entrance velocity. The minimum starting velocities experimentally achieved for the propellant mixtures considered here are listed in Table 1.

In experiments to date the phenomenon which has been observed to limit the maximum attainable velocity in a given propellant mixture has been the eventual "unstarting" of the flow around projectile. One sequence of events which has been observed on a number of occasions, particularly in the high speed, helium-diluted mixtures, is the sudden forward sweep of the shock system on the projectile. This behavior may be a result of either shock ignition of the gases at the rear of the projectile or of combustion rapidly creeping up a separated boundary layer on the back half of the projectile. Typically, this velocity limiting mechanism has been observed to occur in the Mach number range of ~4.0–4.5, depending on the particular propellant mixture.

The maximum velocity experimentally attained with the mixtures investigated to date for the Type A projectile geometry is typically about 85% of the C-J detonation velocity. Enhanced performance at near-detonation velocities has been observed for the Type B projectiles. For example, the upper velocity limit in the $3.5CH_4 + 2O_2 + 6.5He$ mixture for the Type A projectile has been experimentally determined to be 2100 ± 50 m/s. The longer Type B projectile is capable of an upper velocity limit of approximately 2300 m/s in this mixture, i.e., 98% of the C-J detonation velocity. The maximum velocities for the first three mixtures listed in Table 1 were attained with Type B projectiles. The maximum velocity in the fourth mixture was attained with a Type A projectile. The velocity limit of this mixture with the heavier Type B projectile (55–75 gm) has not yet been determined because the length of the existing ram accelerator tube is not sufficient to allow the projectile to reach its ultimate velocity, even at the maximum fill pressure of 35 atm used to date.

The observed increases in maximum velocity with the Type B projectile geometry are believed to be due to more efficient supersonic compression, the longer body on which the normal shock system can stabilize, and the increased separation distance between the normal shock system and the recirculation zone at the base of the projectile. Other factors may be the enhanced projectile stability derived from greater fin length and the reduced divergence angle of the flow behind the throat. The lower divergence angle reduces the adverse pressure gradient, thus reducing the tendency of the boundary layer to separate. Investigations into projectile geometry effects are currently being pursued.

### Transition Between Mixtures

When staged mixtures are used, the transition to a faster mixture, i.e., a mixture whose speed of sound is significantly higher than the previous mixture, involves three key factors. These are the position of the normal shock system on the projectile at transition, the Mach number in the new mixture, and the heat of combustion of the new mixture. As noted earlier, the shock structure observed on the projectile is believed to be a complex wave system consisting of normal and oblique shocks. If this system falls back to the rear of the projectile prior to the transition point, the wave system in the new mixture may initiate a detonation wave that overtakes the projectile, causing its diffuser to unstart and the thrust to become negative. In a similar manner, if the head of the normal shock system is too near the throat at the point of transition, it often sweeps upstream of the throat and again unstarts the diffuser. For a successful transition it has been found that the major pressure rise following the system of reflected conical shocks generated by the nose cone, i.e., the head of the normal shock system (B in Fig. 6), should be approximately at the center of the throat-to-base distance.

Figure 9 shows two pressure traces obtained in a successful transition of a Type A projectile between $2.5CH_4 + 2O_2 + 5.6N_2$ and $4.5CH_4 + 2O_2 + 2He$ at 20 atm. The pressure transducers were, respectively, located 30 cm ahead of and 15 cm beyond the Mylar diaphragm which separated the propellant mixtures. The differences between the two traces are the result of the sudden decrease in Mach number (from 3.95 to 3.27) and the different physical properties of the two gas mixtures. In both cases the pressure reaches its maximum somewhat behind the projectile.

### Thrust Coefficient

Figure 10 shows plots of the thrust coefficient, $F/p_1A$, as a function of projectile velocity for the propellant mixtures discussed here. The curves represent the theory and the plotted points the results for the experiments shown in Figs. 7 and 8. The theoretical values of $F/p_1A$ were computed using the iterative solution method based on the thermochemical data provided by the JANAF tables.[14] The experimental values of the thrust coefficient were determined from the acceleration history of the projectiles and Newton's second law. The accelerations, in turn, were determined by centrally differencing

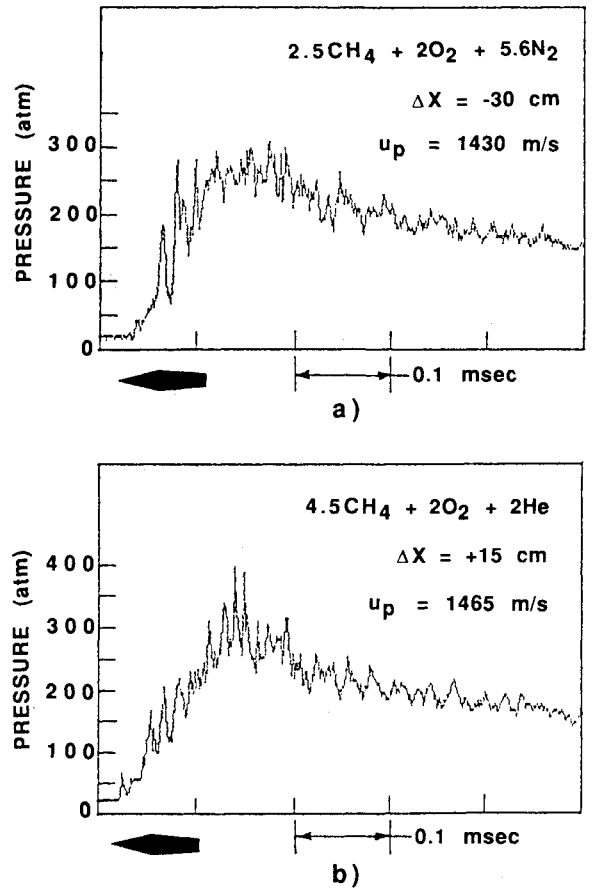


**Fig. 9 Pressure signatures a) before and b) after transition from $2.5CH_4 + 2O_2 + 5.6N_2$ to $4.5CH_4 + 2O_2 + 2He$. Propellant fill pressure = 20 atm; $\Delta x$ refers to locations of pressure transducers with respect to diaphragm which separates the mixtures. Projectile is Type A.**

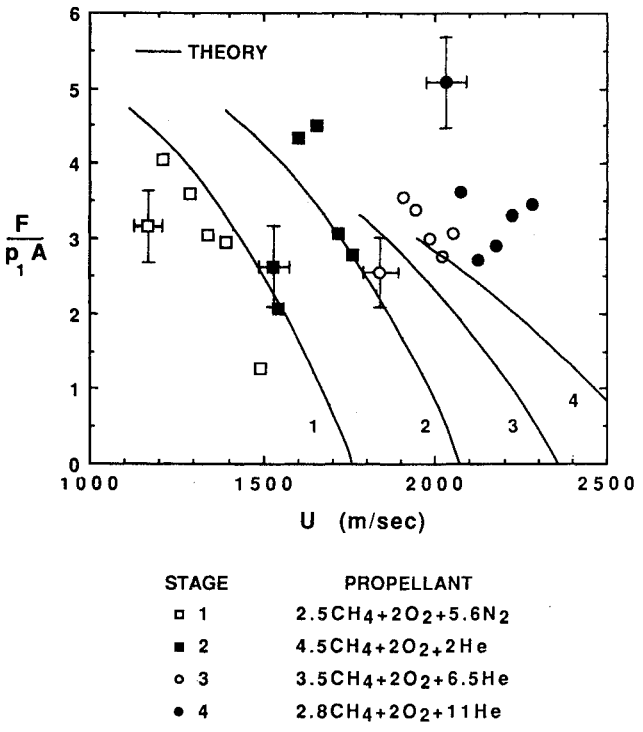


**Fig. 10 Thrust coefficient as a function of velocity for propellant mixtures of Figs. 7 and 8. Curves represent theory. Error bars on first experimental data point in each stage represent the overall probable error from data reduction and experimental uncertainties.**

the experimental $x$-$t$ data and averaging neighboring accelerations to smooth out the variations in the raw distance-acceleration histories. This procedure is preferred over differentiating the curve fit to the experimental data because the trends in performance are not constrained by the order of the polynomial curve fit. The first experimental data point in each stage (see Fig. 10) has a vertical error bar which represents the overall range of probable error in thrust coefficient and a horizontal error bar indicating the uncertainty in velocity at each instrument station. The first stage mixture has experimental values of $F/p_1A$ that increase to a peak value about 10% less than predicted by theory and then decrease with increasing projectile velocity. The second and third stage mixtures have experimental values of the thrust coefficient that straddle the theoretical curves and generally follow the predicted trends. The fourth stage thrust coefficient begins at twice the theoretical prediction, returns to a point about 15% above the curve, and then climbs upward to a final value about 50% above the curve.

The measured thrust coefficients include the frictional drag on the projectile due to both aerodynamic skin friction and wall friction. From test runs without combustion, in which the flow remained supersonic over the entire projectile, the drag coefficient, $D/p_1A$, where $D$ is the drag, was found to be less than 0.01 over the velocity range examined here. Consequently, compared to the measured thrust coefficients in the range of 1.3 to 5.2, the drag coefficient is negligible.

The experimental thrust coefficients observed in the first three stages shown in Fig. 10 are typical of multiple-stage experiments in that the acceleration of the projectile increases when it enters a new mixture and then decreases as the effects of operating at higher Mach numbers reduce its thrust. The behavior of the thrust coefficient in the fourth stage, however, is anomalous in the context of the current model. All the data of this stage lie well above the theoretical curve and beginning at a velocity of about 2150 m/s (~80% of C-J detonation velocity) the thrust coefficient increases as the projectile velocity increases. Based on an examination of the relevant pressure signatures in the fourth stage mixture, the unexpected behavior at the higher velocities may be a result of the normal shock system moving forward on the projectile as the velocity increases. This phenomenon has often been seen when the projectile is allowed to drive up to 80% or more of the mixture detonation velocity, and may be a consequence of chemical energy being transiently released in the reduced flow area around the projectile, as a result of combustion creeping up the boundary layer on the projectile or of shock ignition of the main flow stream. Mixed modes of combustion (subsonic and supersonic) and thermal choking of the flow on the projectile body may also be factors in the deviations of the experiment from the performance predicted by the thermally choked propulsion model. This raises the possibility that a smooth transition to velocities above the C-J detonation velocities of candidate propellant mixtures may be achieved.

## Conclusions

The operational characteristics of a thermally choked, subsonic combustion ram accelerator have been investigated theoretically and experimentally in the velocity range of 1150–2350 m/s, using methane-based propellant mixtures. For typical operating conditions the effect of projectile acceleration on the gasdynamics has been shown to be negligible, so that quasi-steady flow can be assumed. Staged propellant operation and stable transition between different propellant mixtures have been confirmed experimentally. Operational limits in several mixtures have been determined. Projectile velocity increments have been obtained which are consistent with theoretical predictions, and velocities as high as 98% of C-J detonation velocity have been observed. The variation of thrust with projectile velocity is in general agreement with theory at velocities well below the C-J velocity, but is significantly higher than predicted as the C-J velocity is approached. This

anomaly indicates that combustion may be occurring partly on the projectile body and/or that thermal choking may be occurring in the annular region around the projectile. The anomalous behavior raises the possibility that the projectile might be accelerated smoothly to velocities above the C-J velocity within a single propellant mixture. Continued experimentation is needed to answer some of the questions raised in this paper; however, the results to date indicate that the acceleration of projectiles to velocities above 2300 m/s in the thermally choked drive mode can be accomplished with high reliability.

## Acknowledgments

This work was supported in part by USAF Contract FO8635-84-K-0143 and by a grant from the Olin Corporation. The authors are deeply indebted to Alan Kull, Ed Burnham, Kelly Ann Scott, Alfred Alvares and Dai Murakami for their assistance in performing the experiments and to Bill Lowe for his skillful fabrication of the projectiles. In addition, many thanks are due to Walter Christiansen and Keith McFall for their helpful comments on the manuscript.

## References

[1]Hertzberg, A., Bruckner, A. P., and Bogdanoff, D. W., "Ram Accelerator: A New Chemical Method for Accelerating Projectiles to Ultrahigh Velocities," *AIAA Journal*, Vol. 26, 1988, pp. 195–203.

[2]Bruckner, A. P., Bogdanoff, D. W., Knowlen, C., and Hertzberg, A., "Investigation of Gasdynamic Phenomena Associated with the Ram Accelerator Concept," AIAA Paper 87-1327, AIAA 19th Fluid Dynamics, Plasma Dynamics and Lasers Conf., Honolulu, HI, June 8–10, 1987.

[3]Knowlen, C., Bogdanoff, D. W., Bruckner, A. P., and Hertzberg, A., "Performance Capabilities of the Ram Accelerator," AIAA Paper 87-2152, AIAA/SAE/ASME/ASEE 23rd Joint Propulsion Conf., San Diego, CA, June 29–July 2, 1987.

[4]Hertzberg, A., Bruckner, A. P., Bogdanoff, D. W., and Knowlen, C., "The Ram Accelerator and its Applications," *Proceedings of the 16th International Symposium on Shock Tubes and Waves*, Aachen, West Germany, July 26–30, 1987, pp. 117–128.

[5]Bruckner, A. P., Knowlen, C., Scott, K. A., and Hertzberg, A., "High Velocity Modes of the Thermally Choked Ram Accelerator," AIAA Paper 88-2925, AIAA/ASME/SAE/ASEE 24th Joint Propulsion Conf., Boston, MA, July 11–13, 1988.

[6]Brackett, D. C., and Bogdanoff, D. W., "Computational Investigation of Oblique Detonation Ramjet-in-Tube Concepts," *Journal of Propulsion and Power*, Vol. 5, May–June 1989, pp. 276–281.

[7]Yungster, S., and Bruckner, A. P., "A Numerical Study of the Ram Accelerator Concept in the Superdetonative Velocity Range," AIAA Paper 89-2677, AIAA/ASME/SAE/ASEE 25th Joint Propulsion Conf., Monterey, CA, July 10–12, 1989.

[8]Hertzberg, A., Bruckner, A. P., and Bogdanoff, D. W., "A Chemical Method for Achieving Acceleration of Macroparticles to Ultrahigh Velocities, "Final Report UWAERP/15, Department of Enery Contract No. DE-FG06-85ER13382, Aerospace and Energetics Research Program, University of Washington, Seattle, WA, January 1988.

[9]Bruckner, A. P., and Hertzberg, A., "Ram Accelerator Direct Launch System for Space Cargo," 38th Congress of the International Astronautical Federation, Paper No. IAF-87-211, Brighton, England, October 10–17, 1987.

[10]Kaloupis, P., and Bruckner, A. P., "The Ram Accelerator: A Chemically Driven Mass Launcher," AIAA Paper 88-2968, AIAA/ASME/SAE/ASEE 24th Joint Propulsion Conf., Boston, MA, July 11–13, 1988.

[11]Knowlen, C., "Theoretical and Experimental Investigation of the Thermodynamics of the Ram Accelerator in the Thermally Choked Mode," PhD Thesis, Department of Aeronautics and Astronautics, University of Washington, Seattle, WA, April, 1991.

[12]Owczarek, J. A., *Fundamentals of Gas Dynamics*, International Textbook Company, Scranton, PA, 1964, pp. 84–89.

[13]Landau, L. D., and Lifshitz, E. M., *Mechanics*, Addison-Wesley Publishing Co., Reading, MA, 1960, pp. 126–127.

[14]Stull, D. R., and Prophet, H., *JANAF Thermochemical Tables*, 2nd ed, NSRDS-NBS 37, June 1971.

[15]Bogdanoff, D. W., Knowlen, C., Murakami, D., and Stonich, I., "A Magnetic Detector for Projectiles in Tubes," *AIAA Journal*, Vol. 28, 1990, pp. 1942–1944.

[16]Shapiro, A. H., *The Dynamics and Thermodynamics of Compressible Fluid Flows*, Vol. I, Ronald Press, New York, 1953, pp. 135–137.